# Reduced-Rank Adaptive Least Bit-Error-Rate Detection in Hybrid Direct-Sequence Time-Hopping Ultrawide Bandwidth Systems

Qasim Zeeshan Ahmed, Lie-Liang Yang, *Senior Member, IEEE* and Sheng Chen, *Fellow, IEEE*

***Abstract*— Design of high-efficiency low-complexity detection schemes for ultrawide bandwidth (UWB) systems is highly challenging. This contribution proposes a reduced-rank adaptive multiuser detection (MUD) scheme operated in least bit-error-rate (LBER) principles for the hybrid direct-sequence time-hopping UWB (DS-TH UWB) systems. The principal component analysis (PCA)-assisted rank-reduction technique is employed to obtain a detection subspace, where the reduced-rank adaptive LBER-MUD is carried out. The reduced-rank adaptive LBER-MUD is free from channel estimation and does not require the knowledge about the number of resolvable multipaths as well as the knowledge about the multipaths' strength. In this contribution, the BER performance of the hybrid DS-TH UWB systems using the proposed detection scheme is investigated, when assuming communications over UWB channels modeled by the Saleh-Valenzuela (S-V) channel model. Our studies and performance results show that, given a reasonable rank of the detection subspace, the reduced-rank adaptive LBER-MUD is capable of efficiently mitigating the multiuser interference (MUI) and inter-symbol interference (ISI), and achieving the diversity gain promised by the UWB systems.**

***Index Terms*— Ultrawide bandwidth, direct-sequence, time-hopping, adaptive detection, least bit error rate, reduced-rank detection, principal component analysis.**

## I. Introduction

Pulse-based UWB communications schemes constitute a range of promising alternatives that may be deployed for home, personal-area, sensor network, etc. applications, where the communication devices are required to be low-complexity, high-reliability and minimum power consumption [1, 2]. However, in pulse-based UWB systems, the spreading factor is usually very high. The UWB channels are usually very sparse, which results in a huge number of low-power resolvable multipaths [2, 3]. The huge number of resolvable multipaths can provide significant diversity gain, if they are efficiently exploited, but also generates severe MUI and ISI. Hence, in order to attain the promised diversity gain, an UWB receiver has to deal efficiently with the low-power resolvable multipath signals and mitigate the MUI and ISI generated by them. As demonstrated in [1, 3], in pulse-based UWB communications, the huge number of resolvable multipaths generally consist of a few relatively strong paths and many other weak paths. Unlike in the conventional wideband channels where strong paths usually arrive at the receiver before weak paths, in UWB channels, the strong paths are not necessary the ones arriving at the receiver the earliest. In fact, the time-of-arrivals (ToAs) of the strong paths are random variables distributed within a certain range. Due to the above-mentioned issues, therefore, in pulse-based UWB systems, it is normally difficult to implement coherent detection depending on accurate channel estimation. In fact, it has been recognized that, in pulse-based UWB systems, the complexity of the conventional single-user matched-filter (MF) detector [4] might be still too high. This is because the single-user MF detector is a coherent detector, which needs to estimate a huge number of multipath component channels. The complexity of the single-user MF detector is at least proportional to the sum of the spreading factor and the number of resolvable multipaths [5].

In this contribution, we consider the low-complexity detection in hybrid DS-TH UWB systems [6, 7], since the hybrid DS-TH UWB scheme represents a generalized pulse-based UWB communication scheme, including both the pure DS-UWB and pure TH-UWB as its special examples [1, 6, 7]. The detector proposed is an adaptive MUD based on the principles of least bit-error-rate (LBER) [9, 10] operated in a reduced-rank detection subspace. Hence, for convenience, it is referred to as the reduced-rank adaptive LBER-MUD. The reduced-rank subspace, which is also referred to as the detection subspace, is obtained based on the principal component analysis (PCA) [12]. It has a rank that is usually significantly lower than that of the original observation space. As our forthcoming discourse show, the reduced-rank adaptive LBER-MUD does not require channel estimation. At the start of communication, the reduced-rank adaptive LBER-MUD achieves its near-optimum detection with the aid of a training sequence. During communication, it maintains its near-optimum detection based on the decision-directed (DD) principles [11]. Furthermore, the reduced-rank adaptive LBER-MUD does not require the knowledge about the number of resolvable multipaths as well as the knowledge about the locations of the strong resolvable multipaths. It only requires the knowledge, which is still not necessary very accurate, about the maximum delay-spread of the UWB channels. In this contribution, the BER performance of the hybrid DS-TH UWB systems using the proposed reduced-rank adaptive LBER-MUD is investigated, when assuming communications over UWB channels modeled by the Saleh-Valenzuela (S-V) channel model. Our simulation

Q.Z. Ahmed is with The Department of Electrical Engineering, National University of Computer and Emerging Sciences (NUCES-FAST), Islamabad, Pakistan (Email: qasim.zeeshan@nu.edu.pk).

L.-L. Yang and S. Chen are with the School of Electronics and Computer Science, University of Southampton, SO17 1BJ, UK (E-mail: lly, sqc@ecs.soton.ac.uk, http://www-moble.ecs.soton.ac.uk/).

This work was presented in part at the IEEE ICC'2009 , June 14-18 2009, Dresden, Germany.

results show that the reduced-rank adaptive LBER-MUD is capable of suppressing efficiently both the MUI and ISI, and attaining the diversity promised by the UWB channels.

Note that, in this contribution, the LBER algorithm is preferred instead of the conventional least mean-square (LMS) algorithm [13, 14], because of the following observations. First, in terms of the BER performance, the LBER algorithm works under the principles of minimum BER (MBER), which may outperforms the LMS algorithm operated in the principles of minimum mean-square error (MMSE) [9, 10]. This observation is also verified by our simulation results shown in Section IV. Second, the LBER algorithm has a similar complexity as the LMS algorithm [9, 10]. Furthermore, as analyzed in [9, 10], the LBER algorithm can provide a higher flexibility for system design in comparison with the LMS algorithm. Note furthermore that, in [15, 16], the performance of hybrid DS-TH UWB systems employing reduced-rank adaptive detection has been investigated, when the reduced-rank adaptive detectors are operated in the principles of normalized least mean-square (NLMS) [15] or recursive least square (RLS) [16]. The reader who is interested in the details of these reduced-rank adaptive detectors is referred to the above-mentioned references.

The remainder of this paper is organized as follows. Section II describes the system model of the hybrid DS-TH UWB system, which includes transmitted signal, channel model and receiver. In Section III detection of hybrid DS-TH UWB system is addressed. Simulation results are provided in Section IV and, finally, in Section V conclusions of the paper are presented.

## II. Description of the Hybrid DS-TH UWB System

The hybrid DS-TH UWB scheme considered in this paper is the same as that considered in [6, 7, 14, 15]. Specifically, in [6], the BER performance of the hybrid DS-TH UWB system using single-user MF detector and MMSE-MUD has been investigated. In [7, 14], the full-rank adaptive detection has been considered, when the adaptive detector is operated based on the normalized least mean-square (NLMS) [7] or LMS [14] algorithm. Furthermore, in [15, 16], the reduced-rank adaptive detection in hybrid DS-TH UWB systems has been investigated, where the reduced-rank adaptive detectors are operated in the principles of NLMS [15] or RLS [16]. Below we provide a brief description of the hybrid DS-TH UWB system model.

### A. Transmitted Signal

The transmitter schematic block diagram for the considered hybrid DS-TH UWB system is shown in Fig. 1. We assume for simplicity that the hybrid DS-TH UWB system employs the binary phase-shift keying (BPSK) baseband modulation. As shown in Fig. 1, a data bit of the $k$th user is first modulated by a $N_c$-length DS spreading sequence, which generates $N_c$ chips. The $N_c$ chips are then transmitted by $N_c$ time-domain pulses within one symbol-duration, where the positions of the $N_c$ time-domain pulses are determined by the TH pattern assigned to the $k$th user. According to Fig. 1, it can be shown

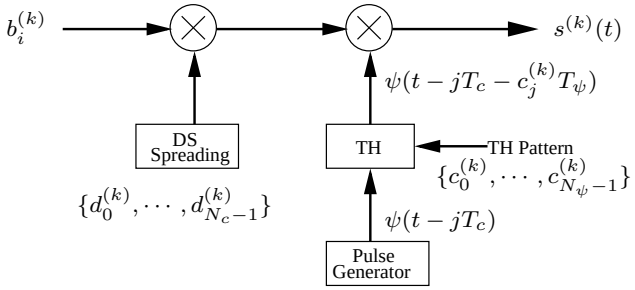


Fig. 1. Transmitter schematic block diagram of the hybrid DS-TH UWB systems.

that the hybrid DS-TH UWB baseband signal transmitted by the $k$th user can be written as [6]

$$s^{(k)}(t) = \sqrt{\frac{E_b}{N_c T_\psi}} \sum_{j=0}^{\infty} b^{(k)}_{\lfloor \frac{j}{N_c} \rfloor} d_j^{(k)} \psi \left[ t - jT_c - c_j^{(k)} T_\psi \right] \quad (1)$$

where $\lfloor x \rfloor$ represents the largest integer less than or equal to $x$, $\psi(t)$ is the basic time-domain pulse of width $T_\psi$, which satisfies $\int_0^{T_\psi} \psi^2(t)dt = T_\psi$. Note that, the bandwidth of the hybrid DS-TH UWB system is approximately equal to the reciprocal of $T_\psi$. The other parameters used in (1) as well as some other related parameters are listed as follows:

- $E_b$: Energy per bit;
- $N_c$: Number of chips per bit, which is the DS spreading factor;
- $N_\psi$: Number of time-slots per chip, which is the TH spreading factor;
- $N_c N_\psi$: Total spreading factor of hybrid DS-TH UWB system.
- $T_b$ and $T_c$: Bit-duration and chip-duration, which satisfy $T_b = N_c T_c$;
- $T_\psi$: Width of time-domain pulse or width of time-slot, which satisfies $T_c = N_\psi T_\psi$;
- $b_i^{(k)} \in \{+1, -1\}$: The $i$th data bit transmitted by user $k$;
- $\{d_j^{(k)}\}$: Random binary DS spreading sequence assigned to the $k$th user;
- $\{c_j^{(k)} \in \{0, 1, \cdots, N_\psi - 1\}\}$: Random TH pattern assigned to the $k$th user.

Note that, the pure DS-UWB and pure TH-UWB schemes are two special examples of the hybrid DS-TH UWB scheme. Specifically, if $N_c > 1$ and $N_\psi = 1$, $T_\psi$ and $T_c$ are then equal and, in this case, the hybrid DS-TH UWB scheme is reduced to the pure DS-UWB scheme. By contrast, when $N_c = 1$ and $N_\psi > 1$, the hybrid DS-TH UWB scheme is then reduced to the pure TH-UWB scheme.

### B. Channel Model

In this contribution, the S-V channel model is considered. Under this channel model, the $k$th user's channel impulse

response (CIR) can be represented as [17]

$$\begin{aligned} h_k(t) &= \sum_{v=0}^{V-1}\sum_{p=0}^{P-1} h_{p,v}^{(k)}\delta(t - T_v - T_{p,v} - \tau_k) \\ &= \sum_{v=0}^{V-1}\sum_{p=0}^{P-1} h_{p,v}^{(k)}\delta(t - T_v - pT_\psi - \tau_k), \\ & k = 1, 2, \ldots, K \end{aligned} \quad (2)$$

where $\tau_k$ takes into account the lack of synchronization among the user signals as well as the transmission delay, $V$ represents the number of clusters and $P$ denotes the number of resolvable multipaths per cluster. Hence, the total number of resolvable multipaths of the UWB channel can be as high as $L = PV$. For simplicity, we assume that $P$ and $V$ are common for all the $K$ users. In (2), $h_{p,v}^{(k)} = |h_{p,v}^{(k)}|e^{j\theta_{p,v}^{(k)}}$ represents the fading gain of the $p$th multipath in the $v$th cluster, where $|h_{p,v}^{(k)}|$ and $\theta_{p,v}^{(k)}$ are assumed to obey the Rayleigh distribution [17] and uniform distribution in $[0, 2\pi)$, respectively, $T_v$ denotes the arrival time of the $v$th cluster while $T_{p,v} = pT_\psi$ is the arrival time of the $p$th multipath in the $v$th cluster. Furthermore, we assume that the average power of a multipath component at a given delay, say at $T_v + T_{p,v}$, is related to the power of the first resolvable multipath of the first cluster through the relation of [17]

$$\begin{aligned} \Omega_{p,v} =& \Omega_{0,0}\exp\left(-\frac{T_v}{\Gamma}\right)\exp\left(-\frac{T_{p,v}}{\gamma}\right), \\ & V = 0, 1, \ldots, V-1;\ p = 0, 1, \ldots, P-1 \end{aligned} \quad (3)$$

where $\Omega_{p,v} = E\left[|h_{p,v}^{(k)}|^2\right]$ represents the power of the $p$th resolvable multipath in the $v$th cluster, $\Gamma$ and $\gamma$ are the cluster and ray power decay constants, respectively.

According to (2), we can know that the maximum delay-spread of the UWB channels considered is $(T_V + T_{P,V})$ and the total number of resolvable multipaths is about $L = \lfloor (T_V + T_{P,V})/T_\psi \rfloor + 1$. In order to make our channel model sufficiently general, in this paper, we assume that the maximum delay spread $(T_V + T_{P,V})$ spans $g \geq 1$ data bits, yielding severe ISI. This also implies that $(g-1)N_cN_\psi \leq (L-1) < gN_cN_\psi$, since the bit-duration is $T_b = N_cN_\psi T_\psi$.

### C. Receiver Structure

When the $K$ number of DS-TH UWB signals in the form of (1) are transmitted over UWB channels having the CIR as shown in (2), the received signal at the base-station (BS) can be expressed as

$$\begin{aligned} r(t) =& \sqrt{\frac{E_b}{N_cT_\psi}}\sum_{k=1}^{K}\sum_{j=0}^{MN_c}\sum_{v=0}^{V-1}\sum_{p=0}^{P-1} h_{p,v}^{(k)} b_{\lfloor \frac{j}{N_c} \rfloor}^{(k)} d_j^{(k)} \\ & \times \psi_{rec}\left[t - jT_c - c_j^{(k)}T_\psi - T_v^{(k)} - T_{p,v}^{(k)} - \tau_k\right] + n(t) \end{aligned} \quad (4)$$

where $n(t)$ represents an additive white Gaussian noise (AWGN) process, which has zero-mean and a single-sided power spectral density of $N_0$ per dimension, $\psi_{rec}(t)$ is the received time-domain pulse, which is usually the second derivative of the transmitted pulse $\psi(t)$ [18].

The receiver schematic block diagram for the hybrid DS-TH UWB systems using the considered reduced-rank adaptive LBER-MUD is shown in Fig. 2. As shown in Fig. 2, the received signal is first filtered by a MF having an impulse response of $\psi_{rec}^*(-t)$. The output of the MF is then sampled at a rate of $1/T_\psi$. The observation samples are first stored in a buffer and then projected onto the reduced-rank detection subspace $\boldsymbol{P}_U$, once it is obtained. Finally, the adaptive LBER-MUD is carried out based on the observations in the detection subspace $\boldsymbol{P}_U$, as detailed in our forthcoming discourse.

Let us assume that a block of data per user containing $M$ number of data bits is transmitted. Then, the receiver can collect a total $(MN_cN_\psi + L - 1)$ number of samples, where $(L-1)$ is due to the $L$ number of resolvable multipaths. In more detail, the $\lambda$th sample can be obtained by sampling the MF's output at the time instant of $t = T_0 + (\lambda+1)T_\psi$, which can be expressed as

$$y_\lambda = \left(\sqrt{\frac{E_bT_\psi}{N_c}}\right)^{-1}\int_{T_0+\lambda T_\psi}^{T_0+(\lambda+1)T_\psi} r(t)\psi_{rec}^*(t)dt \quad (5)$$

where $T_0$ denotes the ToA of the first multipath in the first cluster.

In order to reduce the detection complexity of the hybrid DS-TH UWB system, in this contribution, we consider only the bit-by-bit based detection. Let the observation vector $\boldsymbol{y}_i$ and the noise vector $\boldsymbol{n}_i$ related to the detection of the $i$th data bit of the first user, which is referred to as the reference user, be represented by

$$\boldsymbol{y}_i = [y_{iN_cN_\psi}, y_{iN_cN_\psi+1}, \cdots, y_{(i+1)N_cN_\psi+L-2}]^T \quad (6)$$

$$\boldsymbol{n}_i = [n_{iN_cN_\psi}, n_{iN_cN_\psi+1}, \cdots, n_{(i+1)N_cN_\psi+L-2}]^T \quad (7)$$

where the elements of $\boldsymbol{n}_i$ are Gaussian random variables with zero mean and a variance of $\sigma_n^2 = N_0/2E_b$ per dimension. Then, according to [7, 14], $\boldsymbol{y}_i$ can be expressed as

$$\begin{aligned} \boldsymbol{y}_i =& \underbrace{\sum_{k=1}^{K}\sum_{\substack{j=\max(0,i-g)\\ i\neq 0}}^{i-1}\underline{\boldsymbol{C}}_j^{(k)}\boldsymbol{h}_k\boldsymbol{b}_j^{(k)}}_{\text{ISI from the previous bits of } K \text{ users}} + \underbrace{\boldsymbol{C}_i^{(1)}\boldsymbol{h}_1 b_i^{(1)}}_{\text{Desired signal}} \\ & + \underbrace{\sum_{k=2}^{K}\boldsymbol{C}_i^{(k)}\boldsymbol{h}_k b_i^{(k)}}_{\text{Multiuser interference}} + \underbrace{\sum_{k=1}^{K}\sum_{\substack{j=i+1\\ i\neq M-1}}^{\min(M-1,i+g)}\bar{\boldsymbol{C}}_j^{(k)}\boldsymbol{h}_k\boldsymbol{b}_j^{(k)}}_{\text{ISI from the latter bits of } K \text{ users}} \\ & + \boldsymbol{n}_i \end{aligned} \quad (8)$$

where the matrices and vectors have been defined in detail in [6, 14]. From (8), we are implied that the $i$th data bit of the reference user conflicts both severe ISI and MUI, in addition to the Gaussian background noise. Without mitigating efficiently the ISI and MUI, the diversity gain promised by UWB channels may be overwhelmed by the ISI and MUI. Let us now consider the reduced-rank adaptive LBER-MUD in the next section.

## III. Detection of hybrid DS-TH UWB Signals

First, we note that, when the conventional linear detectors without invoking reduced-rank techniques are considered, the

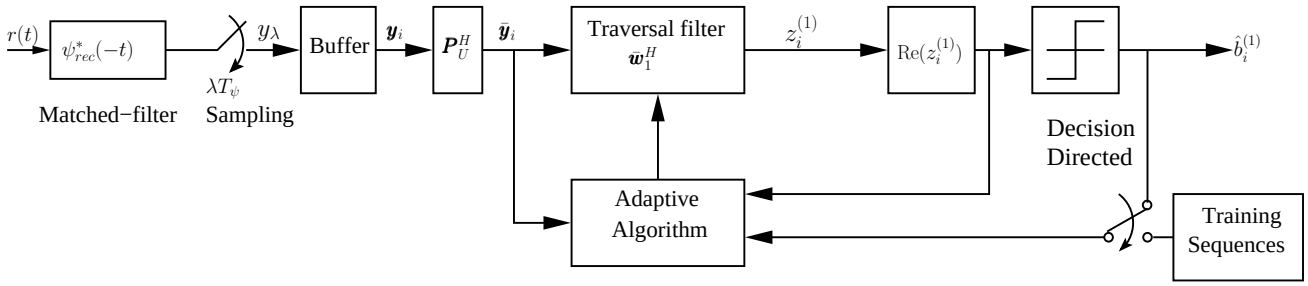


Fig. 2. Receiver schematic block diagram for the hybrid DS-TH UWB systems using reduced-rank adaptive detection.

decision variable for $b_i^{(1)}$ of the reference user can be formed as

$$z_i^{(1)} = \boldsymbol{w}_1^H \boldsymbol{y}_i, \ i = 0, 1, \ldots, M-1 \tag{9}$$

where $\boldsymbol{w}_1$ is a $(N_c N_\psi + L - 1)$-length weight vector. As mentioned previously, in hybrid DS-TH UWB systems, the total spreading factor $N_c N_\psi$ may be very high and the number of resolvable multipaths $L$ of UWB channels is usually very big. Hence, the length of the weight vector $\boldsymbol{w}_1$ or the linear filter's length may be very large. In this case, the complexity of the corresponding detectors might be extreme, even when linear detection schemes are considered. Furthermore, using very long filter for detection in UWB systems may significantly degrade the performance of the UWB systems. For example, using a longer traversal filter results in lower convergence speed and, hence, a longer sequence is required for training the filter [13]. Consequently, the data-rate or spectral efficiency of the corresponding communications systems decreases. The robustness of an adaptive filter also degrades as the filter length increases, since, in this case, more channel-dependent variables are required to be estimated for the filter [19]. Furthermore, when a longer adaptive filter is employed, the computational complexity is also higher, as more operations are required for the corresponding detection and estimation. Therefore, in this contribution, we consider the reduced-rank adaptive MUD, which is operated in the LBER principles, i.e., the reduced-rank adaptive LBER-MUD.

The reduced-rank adaptive LBER-MUD starts with projecting the observation vector $\boldsymbol{y}_i$ onto a lower dimensional subspace referred to as the *detection subspace*, as shown in Fig. 2. Specifically, let $\boldsymbol{P}_U$ be an $((N_c N_\psi + L - 1) \times U)$ processing matrix with its $U$ columns determining an $U$-dimensional detection subspace, where $U < (N_c N_\psi + L - 1)$. Then, given an observation vector $\boldsymbol{y}_i$, the $U$-length vector in the detection subspace can be expressed as

$$\bar{\boldsymbol{y}}_i = \boldsymbol{P}_U^H \boldsymbol{y}_i \tag{10}$$

where an over-bar is used to indicate that the argument is in the reduced-rank detection subspace.

In this contribution, we consider the PCA-assisted reduced-rank technique [12, 20], which derives the processing matrix $\boldsymbol{P}_U$ as follows. First, the auto-correlation matrix $\boldsymbol{R}_{y_i}$ of $\boldsymbol{y}_i$ is estimated based on some training data as

$$\boldsymbol{R}_{y_i} = E[\boldsymbol{y}_i \boldsymbol{y}_i^H] \approx \frac{1}{N} \sum_{i=1}^{N} \boldsymbol{y}_i \boldsymbol{y}_i^H \tag{11}$$

where $N$ denotes the number of data bits invoked for estimating $\boldsymbol{R}_{y_i}$. Then, the auto-correlation matrix $\boldsymbol{R}_{y_i}$ is represented using eigen-analysis as

$$\boldsymbol{R}_{y_i} = \boldsymbol{\Phi} \boldsymbol{\Lambda} \boldsymbol{\Phi}^H \tag{12}$$

where $\boldsymbol{\Lambda}$ is a diagonal matrix containing the eigenvalues of $\boldsymbol{R}_{y_i}$, which can be written as

$$\boldsymbol{\Lambda} = \mathrm{diag}\{\lambda_1, \lambda_2, \cdots, \lambda_{N_c N_\psi + L - 1}\}, \tag{13}$$

while $\boldsymbol{\Phi}$ is an unitary matrix consisting of the eigenvectors of $\boldsymbol{R}_{y_i}$, expressed as

$$\boldsymbol{\Phi} = [\boldsymbol{\phi}_1, \boldsymbol{\phi}_2, \cdots, \boldsymbol{\phi}_{N_c N_\psi + L - 1}] \tag{14}$$

where $\boldsymbol{\phi}_i$ is the eigenvector corresponding to the eigenvalue $\lambda_i$. Finally, let us assume that the eigenvalues are arranged in descent order satisfying $\lambda_1 \geq \lambda_2 \geq \cdots \geq \lambda_{N_c N_\psi + L - 1}$. Then, the processing matrix $\boldsymbol{P}_U$ in the context of the PCA-assisted reduced-rank technique is constructed by the first $U$ columns of $\boldsymbol{\Phi}$, i.e., we have

$$\boldsymbol{P}_U = [\boldsymbol{\phi}_1, \boldsymbol{\phi}_2, \cdots, \boldsymbol{\phi}_U]. \tag{15}$$

Given the observation vector $\bar{\boldsymbol{y}}_i$ as shown in (10), the linear detection of $b_i^{(1)}$ can now be carried out by forming the decision variable

$$z_i^{(1)} = \bar{\boldsymbol{w}}_1^H \bar{\boldsymbol{y}}_i, \tag{16}$$

as shown in Fig. 2. In (16), $\bar{\boldsymbol{w}}_1$ is now an $U$-length weight vector instead of an $(N_c N_\psi + L - 1)$-length vector in (9) for the conventional linear detectors. According to the properties of the PCA-based reduced-rank detection [12], the full-rank BER performance can be attained, provided that the rank $U$ of the detection subspace is not lower than the rank of the signal subspace, which for our hybrid DS-TH UWB system is $K(g+1)$. However, if the rank of the detection subspace is lower than the signal subspace's rank, the reduced-rank detection may then conflict MUI. Consequently, the BER performance of the hybrid DS-TH UWB system using the PCA-based reduced-rank detection deteriorates, in comparison with the BER performance achieved by the corresponding full-rank detectors. Therefore, in the PCA-based reduced-rank

detection, it is desirable to have the knowledge about the signal subspace's rank. Note that, in our simulations considered in Section IV, the signal subspace's rank was estimated through eigen-analysis of the auto-correlation matrix $\boldsymbol{R}_{y_i}$, which was estimated based on (11) with the aid of a block of training data.

As shown in Fig. 2, the weight vector $\bar{\boldsymbol{w}}_1$ in (16) is obtained with the aid of the sample-by-sample adaptive LBER algorithm proposed in [9, 10]. Specifically, the reduced-rank adaptive LBER-MUD is operated in two modes, including the training mode and the DD-mode. When operated in the training mode, the weight vector $\bar{\boldsymbol{w}}_1$ is adapted with the aid of a training sequence known to the receiver. Correspondingly, the update equation in the LBER principle can be formulated as [9]

$$\bar{\boldsymbol{w}}_1(i+1) = \bar{\boldsymbol{w}}_1(i) + \mu \frac{\text{sgn}(b_i^{(1)})}{2\sqrt{2\pi}\rho_n} \exp\left(-\frac{|\Re(z_i^{(1)})|^2}{2\rho_n^2}\right) \bar{\boldsymbol{y}}_i, \quad i = 0, 1, 2, \ldots \tag{17}$$

where $\text{sgn}(x)$ is a sign-function, $\mu$ is the step-size and $\rho_n$ is the so-called kernel width [9]. In the adaptive LBER algorithm, the step-size $\mu$ and the kernel width $\rho_n$ are required to be set appropriately, in order to obtain a high convergence rate as well as a small steady BER misadjustment. Furthermore, it has been observed [9] that the above-mentioned two parameters can provide a higher flexibility for system design in comparison with the adaptive LMS algorithm, which employs only single adjustable parameter of the step-size [13].

After the training stage is completed, the normal data transmission is started. At this stage, the reduced-rank adaptive LBER-MUD is switched to the DD-mode. Under the DD-mode, the data bits detected by the receiver are fed back to the reduced-rank adaptive LBER-MUD, in order to update the weight vector $\bar{\boldsymbol{w}}_1$. To be more specific, during the DD-mode, the update equation for the weight vector $\bar{\boldsymbol{w}}_1$ can be formulated as

$$\bar{\boldsymbol{w}}_1(i+1) = \bar{\boldsymbol{w}}_1(i) + \mu \frac{\text{sgn}(\hat{b}_i^{(1)})}{2\sqrt{2\pi}\rho_n} \exp\left(-\frac{|\Re(z_i^{(1)})|^2}{2\rho_n^2}\right) \bar{\boldsymbol{y}}_i, \quad i = 0, 1, 2, \ldots \tag{18}$$

where $\hat{b}_i^{(1)}$ denotes the estimate to $b_i^{(1)}$.

The convergence behavior of the LBER-MUD is jointly determined by the step-size $\mu$ and kernel width $\rho_n$, as implied in (17) and (18). Generally, if the step-size $\mu$ is increased, the LBER-MUD converges faster, as seen, for example, in Fig. 4. However, using a bigger step-size usually leads to a higher misadjustment after the final convergence. By contrast, as our results in Fig. 5 show, when the other related parameters of the LBER-MUD are fixed, there exists an optimum value for the kernel width $\rho_n$, which results in the lowest BER for a given number of training symbols. Additionally, when the communication environment changes, such as, when the number of users supported changes, the step-size $\mu$ and the kernel width $\rho_n$ may need to be adjusted correspondingly, in order to attain the best performance.

Note that, in comparison with the ideal MMSE-MUD as shown in [6], the reduced-rank adaptive LBER-MUD considered in this contribution employs the following advantages. Firstly, it is free from channel estimation and does not require the knowledge about the user signatures. By contrast, the ideal MMSE-MUD requires channel estimation and all the above-mentioned knowledge. Secondly, operated in the principles of adaptive LBER, the reduced-rank adaptive LBER-MUD does not need to compute the inverse of the auto-correlation matrix $\boldsymbol{R}_{y_i}$. Hence, it may be argued that the reduced-rank adaptive LBER-MUD has a substantially lower complexity and is also more feasible to implement in practice in comparison with the ideal MMSE-MUD, when UWB communications are considered. Additionally, the reduced-rank adaptive LBER-MUD works under the minimum BER principles, which may outperform the MMSE detector in terms of the attainable BER performance.

In comparison with the PCA-assisted reduced-rank adaptive RLS-MUD studied in [16], the reduced-rank adaptive LBER-MUD has a significantly lower complexity. This is because the adaptive LBER-MUD has a similar complexity as the adaptive LMS-MUD [9, 10]. It is well-known that the complexity of the LMS algorithm is much lower than that of the RLS algorithm [13]. Let us now provide our simulation results in the next section.

## IV. Simulation Results and Discussion

In this section, the learning and BER performance of the reduced-rank adaptive LBER-MUD is investigated by simulations. We also compare the performance of the reduced-rank adaptive LBER-MUD with that of the reduced-rank adaptive LMS-MUD, since both of them have similar complexity. In our simulations, the total spreading factor was assumed to be a constant of $N_c N_\psi = 64$, where the DS-spreading factor was set to $N_c = 16$ and the TH-spreading factor was hence $N_\psi = 4$. The normalized Doppler frequency-shift of the UWB channels was fixed to $f_d T_b = 0.0001$. The S-V channel model used in [17] was considered and the channel gains were assumed to obey the Rayleigh distribution. In more detail, the parameters of the S-V channel model used in our simulations are $1/\Lambda = 14.11$ns, $\Gamma = 2.63$ns and $\gamma = 4.58$ns, where $\Gamma$ and $\gamma$ have been defined associated with (3), while $\Lambda$ is the cluster arrival rate [17]. Note that, in the above UWB channel model, both the number of clusters $V$ and the number of resolvable paths per cluster $P$ are variables, when given the total number of resolvable paths $L = VP$. In our simulations, the values of $V$ and $P$ are fixed for one frame duration, while independent from one frame to the next.

Fig. 3 shows the learning curve of the reduced-rank adaptive LBER-MUD for the hybrid DS-TH UWB system supporting $K = 5$ users, when the detection subspace has different ranks of $U = 1,\ 5,\ 10,\ 30$ or $78$. Note that, the BER drawn in Fig. 3 was evaluated by the formula

$$\text{BER} = \frac{1}{T_L} \sum_{n=1}^{T_L} Q\left(\frac{\text{sgn}(b_i^{(1)}(n))\Re(z_i^{(1)}(n))}{\sigma_n^2 \sqrt{\bar{w}_1^H \bar{w}_1}}\right) \tag{19}$$

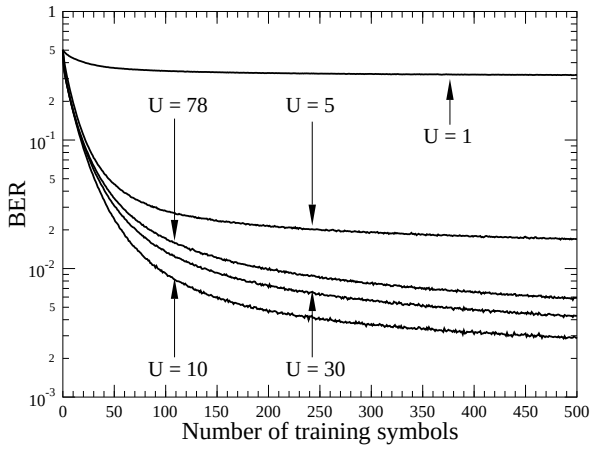


Fig. 3. Learning curves of the reduced-rank adaptive LBER-MUD with respect to different ranks of detection subspaces for the hybrid DS-TH UWB systems supporting $K = 5$ users. The other parameters used in the simulations were $E_b/N_0 = 10$dB, Doppler frequency-shift of $f_dT_b = 0.0001$, $\rho_n = \sigma_n$, $\mu = 0.5$, $g = 1$, $N_c = 16$, $N_\psi = 4$ and $L = 15$.

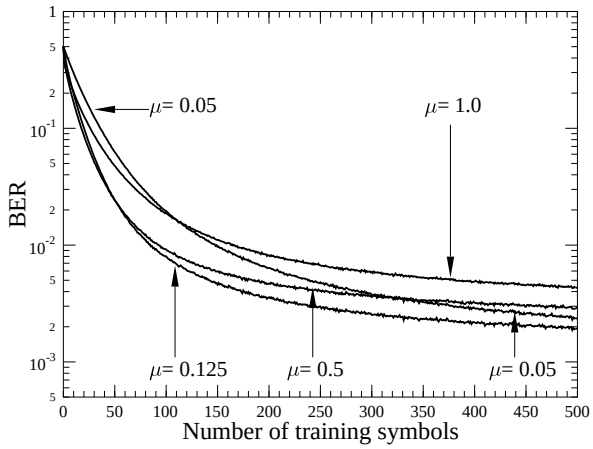


Fig. 4. Learning curves of the reduced-rank adaptive LBER-MUD with respect to different step-size values for the hybrid DS-TH UWB systems supporting $K = 5$ users. The other parameters used in the simulations were $E_b/N_0 = 10$ dB, $f_dT_b = 0.0001$, $U = 10$, $\rho_n = \sigma_n$, $g = 1$, $N_c = 16$, $N_\psi = 4$ and $L = 15$.

where $T_L$ stands for the training length and $Q(x)$ is the Gaussian-$Q$ function defined as

$$Q(x) = \frac{1}{\sqrt{2\pi}} \int_x^\infty \exp\left(-\frac{u^2}{2}\right) du \tag{20}$$

In our simulations, the average signal-to-noise ratio (SNR) per bit was set to $E_b/N_0 = 10$dB, the BER was obtained from the average over $T_L = 100,000$ independent realizations of the UWB channel specified by the parameters $1/\Lambda = 14.11$ns, $\Gamma = 2.63$ns and $\gamma = 4.58$ns. The weight vector was initialized to $\bar{\boldsymbol{w}}_1(0) = \mathbf{1}$ of an all-one vector. Furthermore, we assumed that $g = 1$, implying that the desired bit conflicts ISI from one bit transmitted before the desired bit and also from one bit transmitted after the desired bit. Note that, given the parameters as shown in the caption of the figure, it can be shown that the rank of the signal subspace is $K(g+1) = 10$. From the results of Fig. 3, we observe that, when the rank of the detection subspace is lower than that of the signal subspace, i.e., when $U \leq 10$, the BER performance of the hybrid DS-TH UWB system improves, as the rank of the detection subspace increases. The best BER performance is attained, when the detection subspace reaches the rank of the signal subspace, i.e., when $U = 10$. When the detection subspace uses a rank higher than that of the signal subspace, higher BER is observed. This loss in BER performance is because, in this case, more undesired signals including MUI, ISI and noise are collected by the adaptive LBER-MUD.

Fig. 4 and Fig. 5 illustrate respectively the impact of the step-size $\mu$ and kernel width $\rho_n$ on the learning performance of the reduced-rank adaptive LBER-MUDs for the hybrid DS-TH UWB systems supporting $K = 5$ users, when operated at an average SNR of $E_b/N_0 = 10$ dB. In our simulations for both the figures, the BER was obtained by averaging over $100,000$ independent realizations of the channel. Again, the weight vector was initialized to $\bar{\boldsymbol{w}}(0) = \mathbf{1}$. From the results

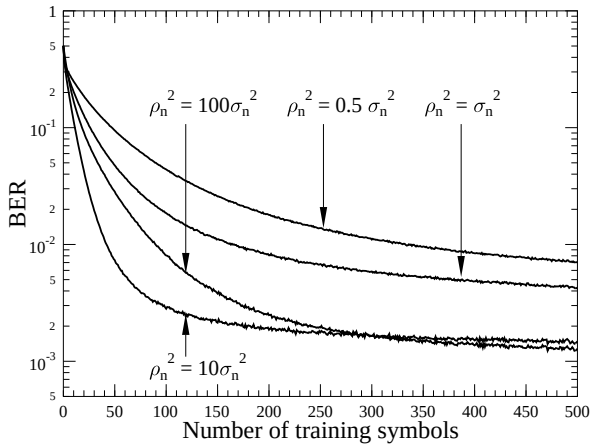


Fig. 5. Learning curves of the reduced-rank adaptive LBER-MUD with respect to different kernel width values for the hybrid DS-TH UWB systems supporting $K = 5$ users. The other parameters used in the simulations were $E_b/N_0 = 10$ dB, $f_dT_b = 0.0001$, $U = 10$, $\mu = 1.0$, $g = 1$, $N_c = 16$, $N_\psi = 4$ and $L = 15$.

of Fig. 4 and Fig. 5, it can be observed that, for a given length of training symbols, an appropriate step-size $\mu$ and an appropriate kernel width $\rho_n$ are usually required, in order for the reduced-rank adaptive LBER-MUD to achieve the lowest BER. Specifically, for the step-size values considered in Fig. 4, the reduced-rank adaptive LBER-MUD using a step-size of $\mu = 0.125$ converges the fastest and also achieves the lowest BER. If the step-size is too low, such as $\mu = 0.05$, or too high, such as $\mu = 1$, the reduced-rank adaptive LBER-MUD may converge with a lower convergence rate but to a higher BER. In the context of the impact from the kernel width $\rho_n$, the results of Fig. 5 imply that there is an optimum kernel width for a given number of training systems. For example,

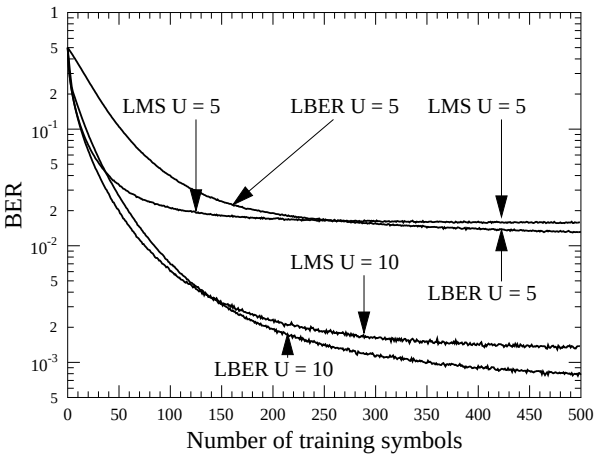


Fig. 6. Learning curves of the reduced-rank adaptive LBER-MUD and LMS-MUD with respect to different ranks of detection subspaces for the hybrid DS-TH UWB systems supporting $K = 5$ users. The other parameters used in the simulations were $E_b/N_0 = 10$ dB, $f_dT_b = 0.0001$, $\mu_{LMS} = 0.001$, $\mu_{LBER} = 0.125$, $\rho_n = \sqrt{10}\sigma_n$,$g = 1$, $N_c = 16$, $N_\psi = 4$ and $L = 15$.

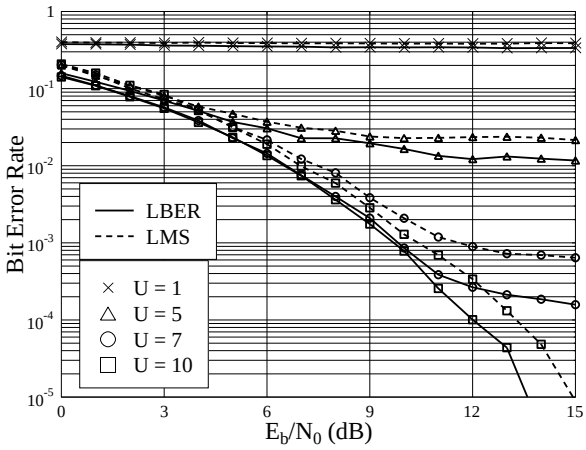


Fig. 7. BER performance of the hybrid DS-TH UWB systems using reduced-rank adaptive LBER- and LMS-MUD, when communicating over the UWB channels modeled by the S-V channel model associated with the parameters $1/\Lambda = 14.11$ns, $\Gamma = 2.63$ns and $\gamma = 4.58$ns. The parameters used in the simulations were $K = 5$, $f_dT_b = 0.0001$, $\mu_{LMS} = 0.001$, $\mu_{LBER} = 0.125$ $\rho_n = \sqrt{10}\sigma_n$, $g = 1$, $N_c = 16$, $N_\psi = 4$ and $L = 15$. The frame length was fixed to 1000 bits, where the first 400 bits were used for training.

when 100 to 150 training symbols are used, the attainable BER first decreases as the value of the kernel width increases, and then increases as the value of the kernel width further increases. Furthermore, for the kernel width values considered in Fig. 5, the reduced-rank adaptive LBER-MUD using $\rho_n^2 = 10\sigma_n^2$ converges with the highest speed. However, when a long training sequence is used, the reduced-rank adaptive LBER-MUD using $\rho_n^2 = 100\sigma_n^2$ may converge to a lower BER.

In Fig. 6, we compare the learning performance of the reduced-rank adaptive LBER-MUD with that of the reduced-rank adaptive LMS-MUD, when the hybrid DS-TH UWB systems operated at an average SNR of $E_b/N_0 = 10$ dB support $K = 5$ users. In our simulations, we set the normalized Dopper frequency-shift to be $f_dT_b = 0.0001$. Furthermore, we assumed that $g = 1$, hence, the desired bit conflicts ISI from one bit transmitted before the desired bit and also from one bit transmitted after the desired bit. Note furthermore that, as discussed associated with Fig. 3, the rank of the signal subspace is $K(g + 1) = 10$. From the results of Fig. 6, we can see that, for a given rank $U$, the LMS-MUD usually converges faster than the LBER-MUD. However, the LBER-MUD is capable of reaching a lower BER than the LMS-MUD. Hence, when having a sufficient number of training symbols, which may be obtained through the techniques such as DD [11], the reduced-rank adaptive LBER-MUD is capable of attaining a lower BER than the reduced-rank adaptive LMS-MUD. Furthermore, the results of Fig. 6 show that, as the rank of the detection subspace is increased from $U = 5$ to $U = 10$, equating the signal subspace's rank, the BER performance of both the detectors is improved significantly.

Fig. 7 shows the BER versus average SNR per bit performance of the hybrid DS-TH UWB systems using either the reduced-rank adaptive LBER-MUD or the reduced-rank adaptive LMS-MUD, when communicating over the UWB channels specified by the parameters $1/\Lambda = 14.11$ns, $\Gamma = 2.63$ns and $\gamma = 4.58$ns. The hybrid DS-TH UWB systems considered supported $K = 5$ users and the normalized Dopper frequency-shift was assumed to be $f_dT_b = 0.0001$. Furthermore, we assumed that the UWB channels had $L = 15$ resolvable paths resulting in $g = 1$. Hence, a desired data bit conflicts ISI from one bit transmitted respectively before and after the desired bit. Note that, given the parameters as shown in the caption of the figure, it can be shown that the rank of the signal subspace is $K(g+1) = 10$. From the results of Fig. 7, we can observe that, when the rank of the detection subspace is lower than that of the signal subspace, i.e., when $U \leq 10$, the BER performance of the hybrid DS-TH UWB system using either the LBER-MUD or the LMS-MUD improves, as the rank of the detection subspace increases. The best BER performance is attained, when the rank of the detection subspace reaches the rank of the signal subspace, i.e., when $U = 10$. When the rank of the detection subspace is lower than that of the signal subspace, error-floors are observed, explaining that the MUI cannot be fully suppressed by the reduced-rank adaptive LBER- and LMS-MUD. Furthermore, for a given rank of the detection subspace, the reduced-rank adaptive LBER-MUD outperforms the reduced-rank adaptive LMS-MUD, in terms of their attainable BER.

Finally, in Fig. 8, we compare the BER versus average SNR per bit performance of the hybrid DS-TH UWB systems using either the reduced-rank adaptive LBER-MUD or reduced-rank adaptive LMS-MUD, when communicating over the UWB channels specified by the parameters $1/\Lambda = 14.11$ns, $\Gamma = 2.63$ns and $\gamma = 4.58$ns. In our simulations we assumed that the UWB channel had $L = 150$ resolvable paths, which hence resulted in severe ISI. Specifically, in contrast to Fig. 7, where the number of resolvable multipaths was $L = 15$ resulting in $g = 1$, the $L = 150$ resolvable paths in Fig. 8 resulted in $g = 3$. The other parameters used for Fig. 8 were the

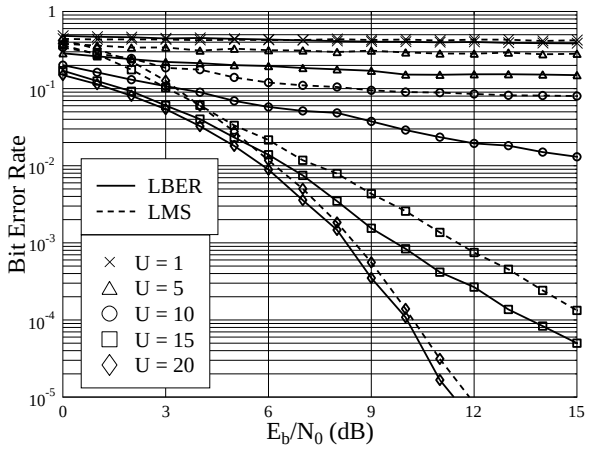


Fig. 8. BER performance of the hybrid DS-TH UWB systems using reduced-rank adaptive LBER- and LMS-MUD, when communicating over the UWB channels modeled by the S-V channel model associated with the parameters $1/\Lambda = 14.11$ns, $\Gamma = 2.63$ns and $\gamma = 4.58$ns. The parameters used in the simulations were $K = 5$, $f_d T_b = 0.0001$, $\mu_{LMS} = 0.5$,$\mu_{LBER} = 0.5$, $\rho_n = \sqrt{100}\sigma_n$, $g = 3$, $N_c = 16$, $N_\psi = 4$ and $L = 150$. The frame length was fixed to 1000 bits, where the first 400 bits were used for training.

same as those used for Fig. 7, as shown in the caption of the figure. Note that, for the parameters considered in Fig. 8, the rank of the signal subspace is $K(g+1) = 20$. Again, as the results of Fig. 8 shown, the BER performance improves as the rank of the detection subspace increases, until it reaches the rank of the signal subspace. In comparison with Fig. 7, we can see that, for a given $E_b/N_0$ value, the full-rank BER shown in Fig. 8 is lower than the corresponding full-rank BER shown in Fig. 7. This is because the UWB channel considered associated with Fig. 8 has $L = 150$ number of resolvable multipaths, which results in a higher diversity gain than the UWB channel considered associated with Fig. 7, which has $L = 15$ number of resolvable multipaths. Furthermore, as observed in Fig. 7, for a given rank of detection subspaces, the reduced-rank adaptive LBER-MUD outperforms the reduced-rank adaptive LMS-MUD, in terms of their attainable BER.

Finally, as an example, in Table. I shown below, we compare the performance and complexity of the proposed algorithm with the correlation detector, MMSE detector, full-rank LMS adaptive detector, full-rank RLS adaptive detector and reduced-rank RLS adaptive detector, when $K = 5$, $N_c = 16$, $N_\psi = 4$, $g = 1$, $L = 15$ and $E_b/N_0 = 10$ dB. The principles of these related detectors can be found in [6, 7, 14–16].

From the Table, we can have the following observations. First, the BER performance of the correlation detector is worse than that of all the other detectors, while the complexity of the correlation detector is lower than that of all the other detectors, except that of the LMS-adaptive MMSE-MUD. Second, the best BER performance is achieved by the ideal MMSE-MUD. However, the number of operations required by the ideal MMSE-MUD is extremely higher than that of the others. Furthermore, for the ideal MMSE-MUD, the knowledge about the signature sequences and channel state information (CSI)

| Algorithm | Rank | BER | No. of Oper. |
|---|---|---|---|
| Correlation detector | 78 | 0.0064307 | 2496 |
| Full-rank ideal MMSE | 78 | 0.00049017 | 267384 |
| Full-rank LMS adaptive | 78 | 0.0039017 | 392 |
| Full-rank RLS adaptive | 78 | 0.0016025 | 67551 |
| PCA-based reduced-rank LMS adaptive detector | 10 | 0.00129 | 8011 |
| PCA-based reduced-rank RLS adaptive detector | 10 | 0.00080188 | 9132 |
| PCA-based reduced-rank LBER adaptive detector | 10 | 0.00078458 | 8014 |

TABLE I
BER PERFORMANCE AND NUMBER OF OPERATIONS REQUIRED TO DETECT ONE BIT.

of all the users is required. Since the exact CSI is usually extremely hard to acquire in UWB communications, the ideal MMSE-MUD is therefore not a desired detector for achieving low-complexity detection in UWB systems. Third, the full-rank LMS-adaptive detector has the lowest complexity. However, its BER performance is only better than that of the correlation detector but far worse than that of the ideal MMSE-MUD. Forth, the BER performance of the full-rank RLS-adaptive detector is better than that of the full-rank LMS-adaptive detector and also better than that of the correlation detector. However, the BER performance is still much worse than that of the ideal MMSE-MUD. Furthermore, the number of operations required by the full-rank RLS-adaptive detector to detect a bit is very high as compared to the full-rank LMS adaptive detector and correlation detector, although it is much lower than that of the ideal MMSE-MUD. Fifth, the BER performance of the reduced-rank adaptive detector is better than that of the full-rank adaptive detector. Moreover, the complexity of the reduced-rank LMS-adaptive detector is higher than that of the full-rank LMS adaptive detector. By contrast, the complexity of the reduced-rank RLS-adaptive detector is lower than that of the full-rank RLS-adaptive detector. Finally, the BER performance of the reduced-rank adaptive LBER-MUD is better than that of all the other reduced-rank and full-rank adaptive detectors. It can also be observed that the reduced-rank RLS-adaptive MMSE-MUD has approximately the same BER performance as the reduced-rank adaptive LBER-MUD. However, the complexity of the reduced-rank RLS-adaptive detector is slightly higher than that of the reduced-rank adaptive LBER-MUD. Furthermore, the reduced-rank adaptive LBER-MUD's BER performance is not far away from that of the ideal MMSE-MUD, but its complexity is much lower than that of the ideal MMSE-MUD.

## V. CONCLUSIONS

In this contribution, we have investigated the learning and achievable BER performance of the hybrid DS-TH UWB systems using reduced-rank adaptive LBER-MUD, when communicating over the UWB channels experiencing both MUI and ISI in addition to multipath fading. Furthermore, comparisons have been made between the reduced-rank adaptive LBER-MUD and the reduced-rank adaptive LMS-MUD in

terms of their learning and achievable BER performance. Our studies and simulation results show that the reduced-rank adaptive LBER-MUD constitutes one of the efficient detectors for the hybrid DS-TH UWB systems. The reduced-rank technique can be employed for achieving low-complexity detection in the DS-TH UWB systems and also for improving their efficiency. The reduced-rank adaptive LBER-MUD is capable of achieving the full-rank BER performance with the detection subspace having a rank that is significantly lower than $(N_c N_\psi + L - 1)$ of the original observation space. Given a rank of the detection subspace, the reduced-rank adaptive LBER-MUD outperforms the reduced-rank adaptive LMS-MUD, in terms of their attainable BER performance. Furthermore, the reduced-rank adaptive LBER-MUD can provide us more degrees-of-freedom for design when compared to the reduced-rank adaptive LMS-MUD with the same level of complexity.

## REFERENCES


[1] J. H. Reed, *An Introduction to Ultra Wideband Communication Systems*. Prentice Hall, 2005.

[2] J. Zhang, P.V. Orlik, Z. Sahinoglu, A.F. Molisch and P. Kinney, "UWB systems for wireless sensor networks," *Proceedings of the IEEE*, vol. 97, pp. 313 - 331, Feb. 2009.

[3] A. F. Molisch, J. R. Foerster, and M. Pendergrass, "Channel models for ultrawideband personal area networks," *IEEE Wireless Communications*, vol. 10, pp. 14–21, Dec. 2003.

[4] S. Verdu, *Multiuser Detection*. Cambridge University Press, 1998.

[5] Q. Li and L. A. Rusch, "Multiuser detection for DS-CDMA UWB in the home environment," *IEEE Journal on Selected Areas in Communications*, vol. 20, pp. 1701–1711, Dec. 2002.

[6] Q. Z. Ahmed and L.-L. Yang, "Performance of hybrid direct-sequence time-hopping ultrawide bandwidth systems in Nakagami-$m$ fading channels," in *IEEE 18th International Symposium on Personal, Indoor and Mobile Radio Communications (PIMRC'07)*, Athens, Greece, pp. 1–5, Sept. 2007.

[7] Q. Z. Ahmed and L.-L. Yang, "Normalised least mean-square aided decision-directed adaptive detection in hybrid direct-sequence time-hopping UWB systems," in *IEEE 68th Vehicular Technology Conference (VTC2008-Fall)*, Calgary, Canada, pp. 1-5, Sept. 2008.

[8] W. Chen and U. Mitra, "Reduced-rank detection schemes for DS-CDMA communication systems," in *IEEE Military Communications Conference (MILCOM)*, vol. 2, Washington, D.C., pp. 1065–1069, Oct. 2001.

[9] S. Chen, S. Tan, L. Xu, and L. Hanzo, "Adaptive minimum error-rate filtering design: A Review," *Signal Processing*, vol. 88, no. 7, pp. 1671–1679, July 2008.

[10] S. Chen, A. K. Samingan, B. Mulgrew, and L. Hanzo, "Adaptive minimum-BER linear multiuser detection for DS-CDMA signals in multipath channels,"*IEEE Transactions on Signal Processing*, vol. 49, no. 6, pp. 1240-1247, June 2001.

[11] R. Kumar, "Convergence of a decision-directed adaptive equalizer," in *22nd IEEE Conference on Decision and Control*, vol. 22, pp. 1319–1324, Dec. 1983.

[12] H. L. V. Trees, *Optimum Array Processing*. Wiley Interscience, 2002.

[13] S. Haykin, *Adaptive Filter Theory*. Prentice Hall, 4 ed., 2002.

[14] Q. Z. Ahmed, W. Liu, and L.-L. Yang, "Least mean square aided adaptive detection in hybrid direct-sequence time-hopping ultrawide bandwidth systems," in *IEEE 67th Vehicular Technology Conference (VTC2008-Spring)*, Marina Bay, Singapore, pp. 1062–1066, May 2008.

[15] Q. Z. Ahmed and L.-L. Yang, "Low-complexity reduced-rank adaptive detection in hybrid direct-sequence time-hopping ultrawide bandwidth systems," in *IEEE 69th Vehicular Technology Conference (VTC2008-Spring)*, Barcelona, Spain, June 2009.

[16] Q. Z. Ahmed and L.-L. Yang, "Reduced-rank adaptive multiuser detection in hybrid direct-sequence time-hopping ultrawide bandwidth systems," *IEEE Transactions on Wireless Communications*, vol. 9, pp. 156-167, Jan. 2010.

[17] J. Karedal, S. Wyne, P. Almers, F. Tufvesson, and A. F. Molisch, "Statistical analysis of the UWB channel in an industrial environment," in *IEEE 60th Vehicular Technology Conference (VTC2004)*, vol. 1, (Los Angeles, CA), pp. 81–85, Sept. 2004.

[18] J. Zhang, T. D. Abhayapala, and R. A. Kennedy, "Role of pulses in ultra wideband systems," in *IEEE International Conference on Ultra-Wideband*, Zurich, Switzerland, pp. 565–570, Sept. 2005.

[19] M. Honig and M. K. Tsatsanis, "Adaptive techniques for multiuser CDMA receivers," *IEEE Signal Processing Magazine*, vol. 17, pp. 49–61, May 2000.

[20] G. H. Dunteman, *Principal Components Analysis*. Newbury Park, 1989.


**Dr. Qasim Zeeshan Ahmed received his B.Eng. degree in Electrical Engineering from the National University of Sciences and Technology (NUST), Rawalpindi, Pakistan in 2001, MSc degree from the University of Southern California (USC) Los-Angeles, USA in 2005 and his PhD degree from the University of Southampton, UK in 2009. Currently, he works as an assistant professor at the National University of Computer and Emerging Sciences (NU-FAST) Islamabad, Pakistan. His research interests include mainly low-complexity UWB transceiver design, adaptive signal processing and spread-spectrum communications.**

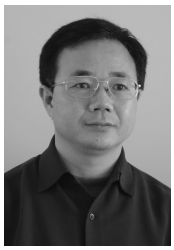

**Lie-Liang Yang (M'98, SM'02) received his BEng degree in communications engineering from Shanghai TieDao University, Shanghai, China in 1988, and his MEng and PhD degrees in communications and electronics from Northern (Beijing) Jiaotong University, Beijing, China in 1991 and 1997, respectively. From June 1997 to December 1997 he was a visiting scientist of the Institute of Radio Engineering and Electronics, Academy of Sciences of the Czech Republic. Since December 1997, he has been with the University of Southampton, United Kingdom, where he is the professor of wireless communications in the School of Electronics and Computer Science. Dr. Yang's research has covered a wide range of topics in wireless communications, networking and signal processing. He has published over 260 research papers in journals and conference proceedings, authored/co-authored three books and also published several book chapters. The details about his publications can be found at http://www-mobile.ecs.soton.ac.uk/lly/. He is currently an associate editor to the *IEEE Transactions on Vehicular Technology*, *Journal of Communications and Networks* (JCN) and the *Security and Communication Networks (SCN) Journal*.**

**Sheng Chen** received his PhD degree in control engineering from the City University, London, UK, in September 1986. He was awarded the Doctor of Sciences (DSc) degree by the University of Southampton, Southampton, UK, in 2005.

From October 1986 to August 1999, he held research and academic appointments at the University of Sheffield, the University of Edinburgh and the University of Portsmouth, all in UK. Since September 1999, he has been with the School of Electronics and Computer Science, University of Southampton, UK.

Professor Chen's research interests include wireless communications, adaptive signal Processing for communications, machine learning, and evolutionary computation methods. He has published over 400 research papers.

Dr Chen is a Fellow of IET and a Fellow of IEEE. In the database of the world's most highly cited researchers, compiled by Institute for Scientific Information (ISI) of the USA, Dr. Chen is on the list of the highly cited researchers in the engineering category.